DEPARTMENT OF THE INTERIOR
U.S. GEOLOGICAL SURVEY

Analysis of a Seismic Anomaly in Georges Bank Basin, Atlantic Continental Margin

by

W.F. Agena[1] and M.W. Lee[1]

U.S. Geological Survey
Open-File Report 91-382

[1] U.S. Geological Survey, Box 25046, Denver Federal Center, Denver, CO 80225

1991

Table of Contents

Figures

Tables

Analysis of a Seismic Anomaly in Georges Bank Basin, Atlantic Continental Margin

by

W.F. Agena and M.W. Lee

Abstract

True-amplitude (TA) processing, wavelet analysis and seismic inversion were used to investigate a 3 km long seismic anomaly observed on USGS line 12 which was shot over the Georges Bank Basin, southeast of New England. Detailed analysis of the surface seismic data and of well data obtained in 1981, indicates that the anomaly is a seismic expression of a remnant volcanic cone underlain by a volcanic intrusive. Efforts to use surface seismic data alone to distinguish between this anomaly and a second anomaly in the area known to be a salt intrusive, proved to be feasible based on the large differences in amplitude. Modeling showed that with amplitude versus offset analysis alone, differentiating between the two anomalies would be marginal at best.

Introduction

Between 1973 and 1978, the U.S. Geological Survey acquired more than 50 marine, multichannel seismic reflection lines over the Atlantic continental shelf. One of the strike lines, USGS line 12 (Figure 1), recorded across the northern section of Georges Bank Basin reveals two seismic anomalies.

Anderson and Taylor (1981) and Lee and others (1991) used detailed seismic analysis to study a unique, 9 km wide, 130 m thick, high-amplitude seismic anomaly. This anomaly, shown in Figure 2, between common midpoints (CMP) 22450 and 22700 at about 2.6 seconds consists of two low-impedance layers separated by laterally thinning high-impedance layers and was interpreted by Lee and others (1991) to be a salt intrusion.

A second, smaller anomaly (about 3 km wide and 341 m thick) appears in Figure 2 as a stratigraphic high between CMPs 21900 and 22000 at about 2.5 seconds. This smaller anomaly was drilled by Exxon in 1981 and was shown to be a remnant volcanic cone of Middle Jurassic age underlain by an Early Cretaceous volcanic intrusive (Hurtubise and others, 1987).

This study is an attempt to seismically characterize the volcanic intrusive and to determine if it can be distinguished seismically from the salt intrusion described by Lee and others (1991). This study is based mainly on the stacked seismic data because the lack of detailed source- and hydrophone- array information and non-uniform channel sensitivity, precluded the use of more up-to-date lithology delineating methods such as amplitude versus offset (AVO) analysis (Backus, 1987).

Geologic setting

Directly southeast of the New England coast along the Atlantic Continental Shelf, and just landward of the East Coast Magnetic Anomaly (ECMA), lies the Georges Bank basin. The Georges Bank region is part of a passive continental margin that formed during Mesozoic time as the coasts

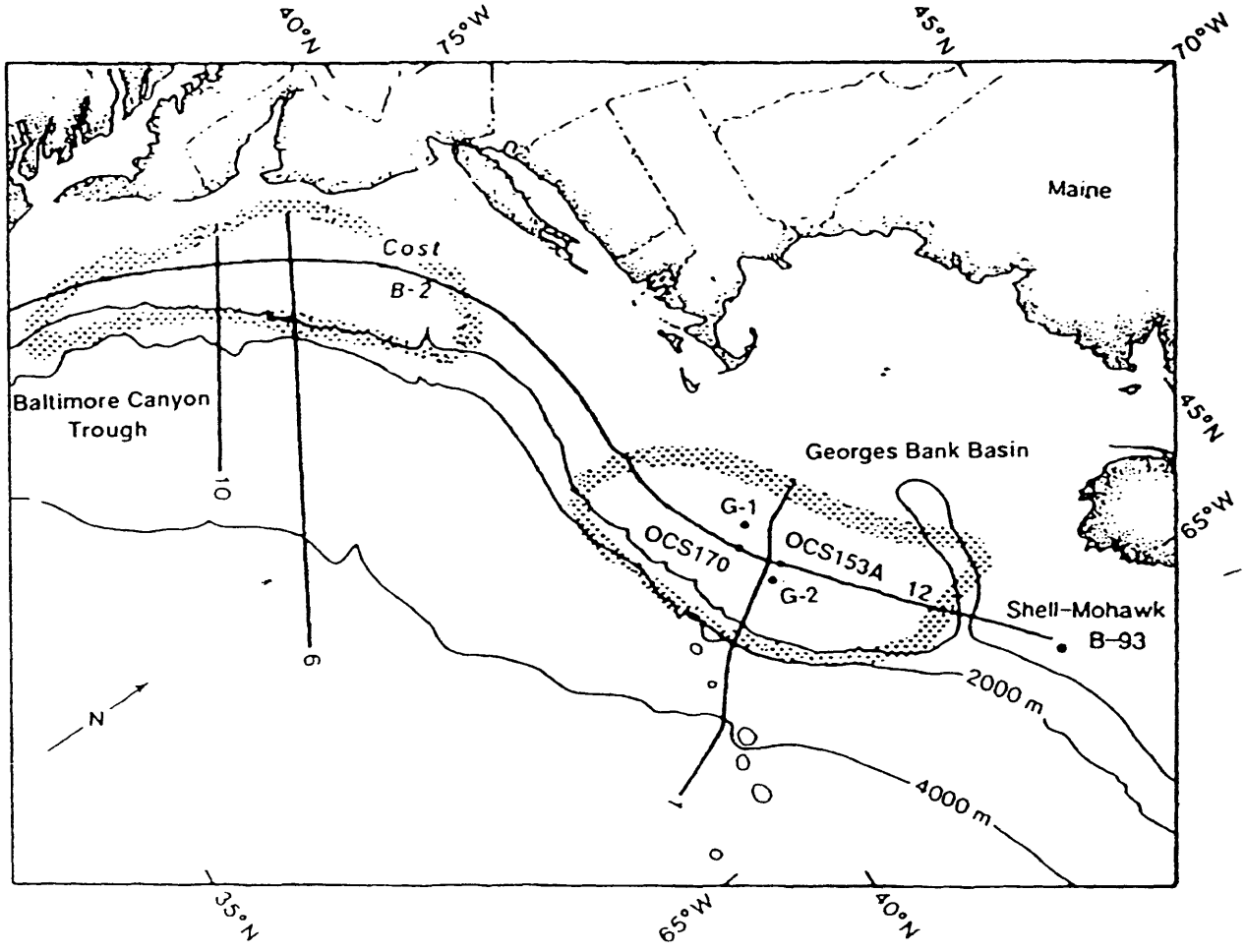

Figure 1.--Location map of study area. Dotted areas delineate the Baltimore Canyon Trough and the Georges Bank Basin.

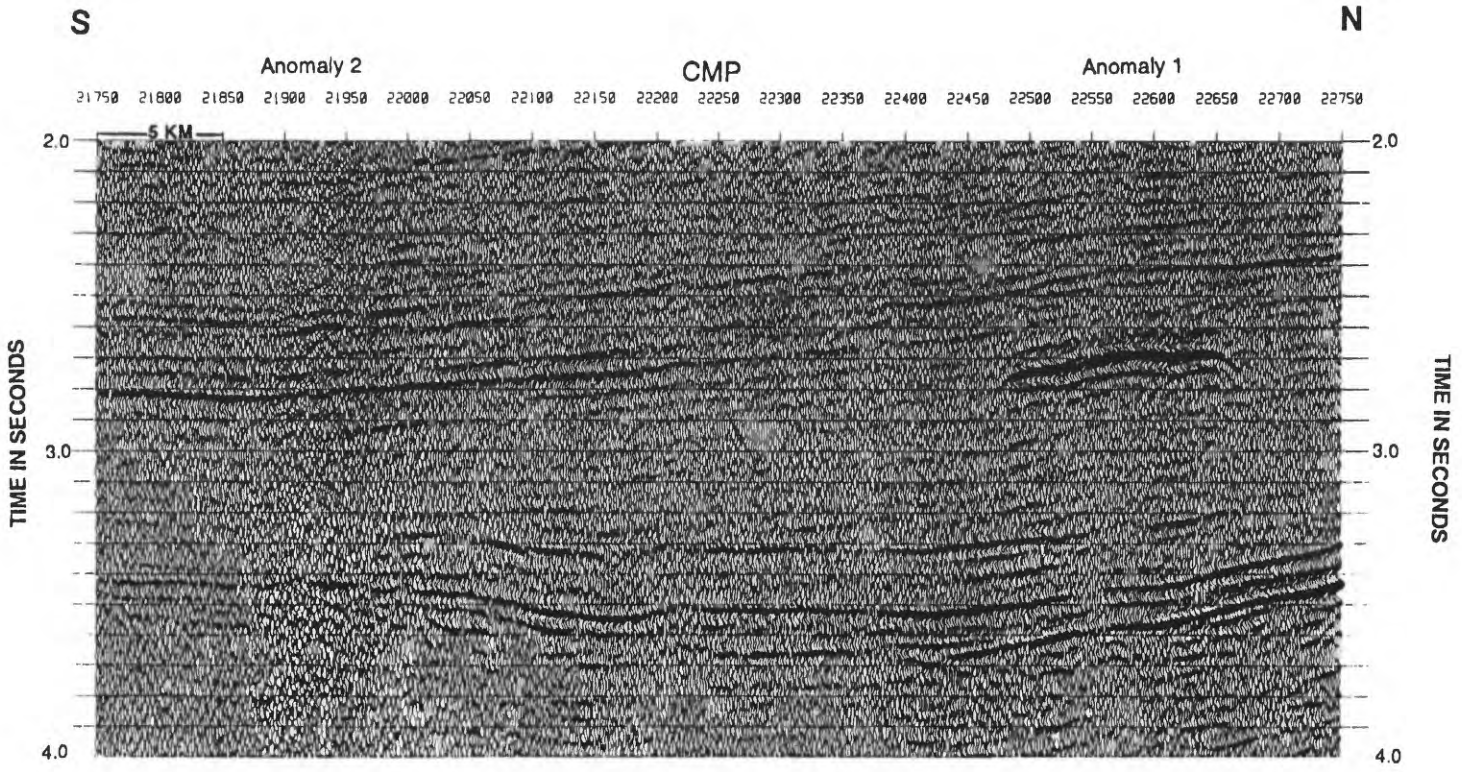

Figure 2.--True-amplitude processed section showing anomalies caused by an intrusive salt layer between CMPs 22450 and 22700 at about 2.6 seconds, and a volcanic sequence between CMPs 21900 and 22000 at about 2.5 seconds.

of present day New England and Morocco began breaking apart (rifting) and then spreading (drifting) (Manspeizer and others, 1978). The region is made up of several small synrift sub-basins, overlying a block-faulted crystalline basement and these smaller sediment-filled sub-basins are in turn overlain by a postrift sedimentary sequence (shown as a schematic in Figure 3). Total sedimentary thickness in some areas of the basin exceeds 10 km.

Schlee and others (1975) proposed that during Triassic time the outer shelf edge acted as a circulation barrier thus creating a shallow marine environment in Georges Bank Basin. Schlee and others (1976, 1977) suggested that in periods of lesser circulation, favorable sea levels, and semi-arid to arid climates, thick accumulations of limestone, dolomite, anhydrite and other evaporites could have been deposited within the basin throughout the Middle Jurassic.

Simonis (1980), Jansa and Wiedmann (1982), and Poag (1982) inferred from tuffs sampled from various drill holes in the basin, that episodes of Middle to Late Jurassic volcanic activity probably occurred contemporaneously with the rifting and subsequent drifting.

Data Acquisition and Processing

The data from line 12 were recorded under contract to the USGS by DIGICON Geophysical Corp. in 1975. Recording parameters included using 100 m shotpoint intervals, and a cable with 48 non-linearly spaced hydrophone groups spaced over 3848 m, resulting in 48-fold common midpoint (CMP) coverage. A 1700 in^3 tuned airgun array was used as the source, and the data were recorded with a DFS-III system sampling at 2 ms intervals.

We first processed the data set using conventional processing methods, including automatic gain control (AGC) to get detailed structural information and to optimize our processing parameters. The data were then reprocessed to preserve true relative amplitudes and waveform characteristics using the processing flow shown in Figure 4. To preserve relative vertical amplitude variation, a constant gain proportional to $T^{1.5}$ was applied to to compensate for spherical divergence and attenuation loss. Lateral amplitude variations recorded in the time-offset (T-X) domain which were caused by changes in recording conditions were corrected by an automatic editing algorithm developed by Lee and Hutchinson (1990). In order to analyze the waveform characteristics, we used the variable norm deconvolution method described by Gray (1979) to estimate the source wavelet, and then design and apply an inverse filter. Extremely shallow water depths in the area prevented us from extracting the wavelet there. We opted to use a section of USGS line 6 (Figure 1) recorded over deeper water and using identical recording parameters, to extract the source wavelet. Originally we intended to incorporate amplitude versus offset (AVO) analysis (Backus,1987) in our study to delineate lithologies from the seismic data. However, analysis performed early in the processing showed that data quality varied significantly between channels and that the far-24 traces were so contaminated by noise that AVO analysis could not be performed with any confidence.

Well Log Analysis

Figure 5 shows data collected from various geophysical logs from well OCS170-A (EXXON 133-1) between 12000 and 14000 ft. Based on well logs, core samples, and well cuttings, volcanic activity is associated with intervals **A-A'** and **B-B'**. Based on both relative (palynologic) and absolute (K-Ar) dating methods, Hurtubise and others (1987) identified the **A-A'** sequence as a Middle Jurassic extrusive event and the **B-B'** sequence as an Early Cretaceous intrusive event. Cross-plots between sonic and density log values (Figure 6) show the **A-A'** interval has a mean density of about 2.65 g/cc and an average velocity of 4.4 km/s (14291 ft/s). The **B-B'** interval has a mean density value of about 2.7 g/cc with velocities averaging about 6.2 km/s (20,446 ft/s). Densities for the limestone intervals above, below, and between the anomalous zones are about 2.7 g/cc and their velocities average about 5.7 km/s (18,900 ft/s).

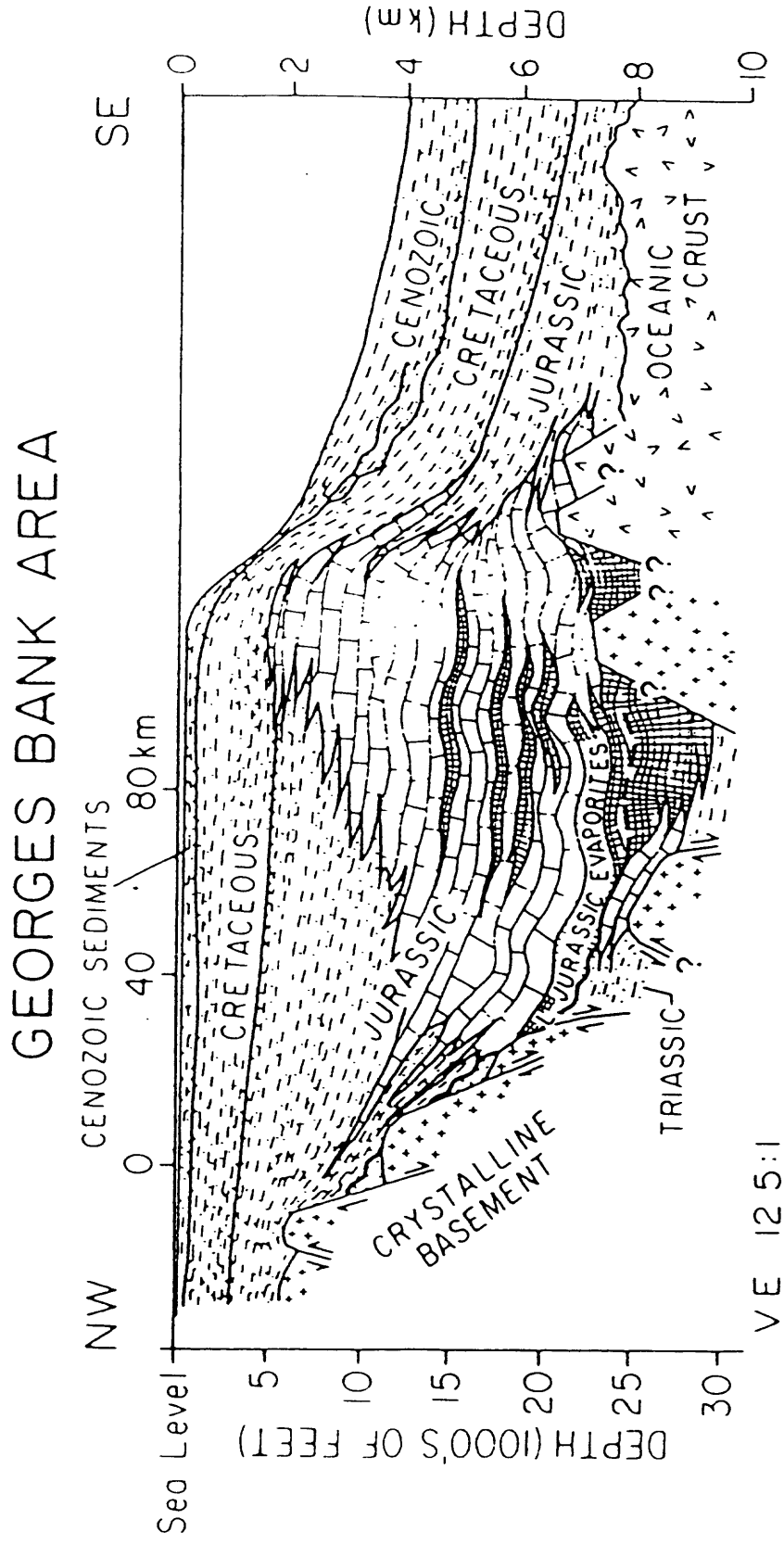

Figure 3.--A cross-section schematic of the Georges Bank Basin (From Schlee & Klitgord, 1981)

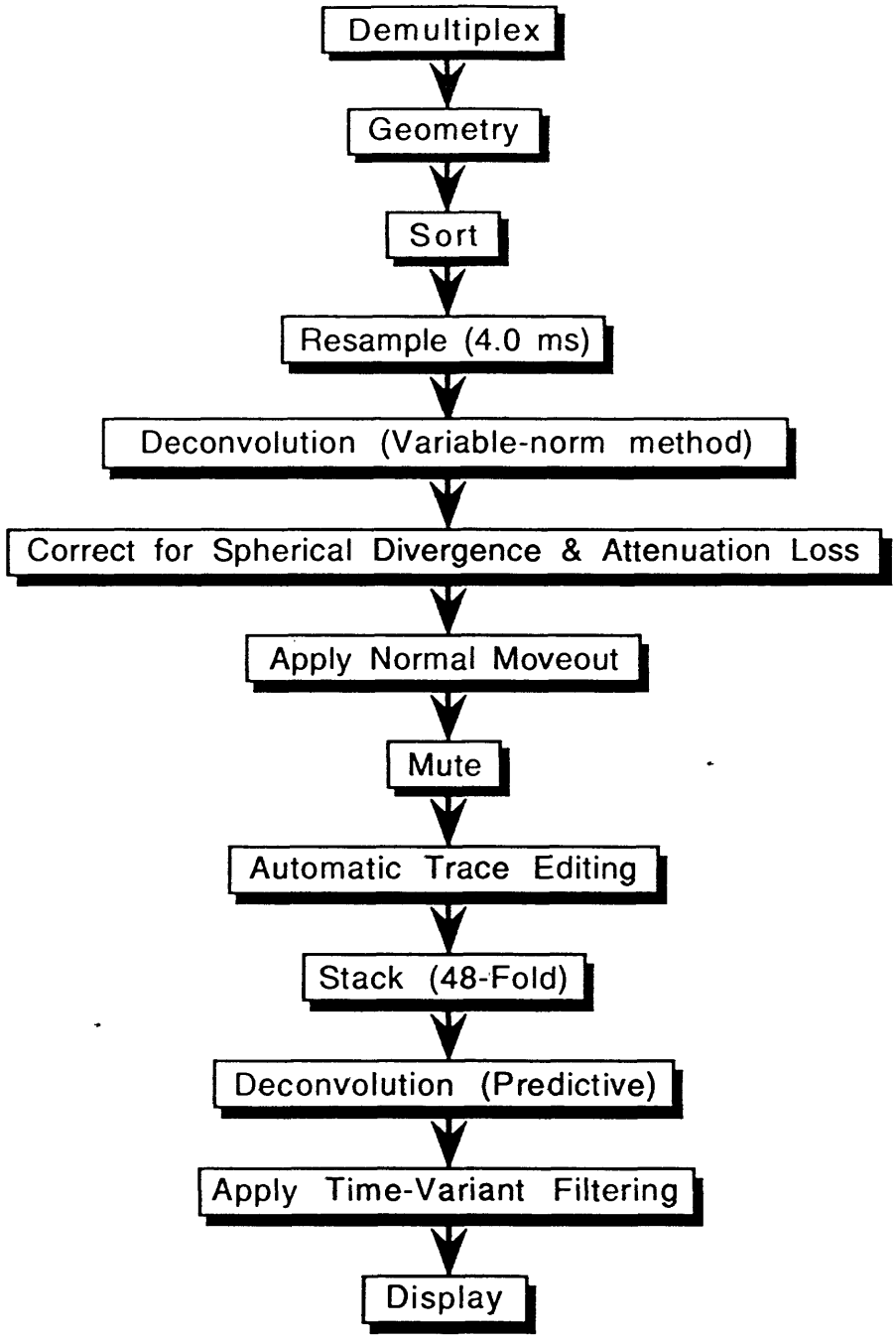

Figure 4.--Flow diagram of the processing sequence used in the study.

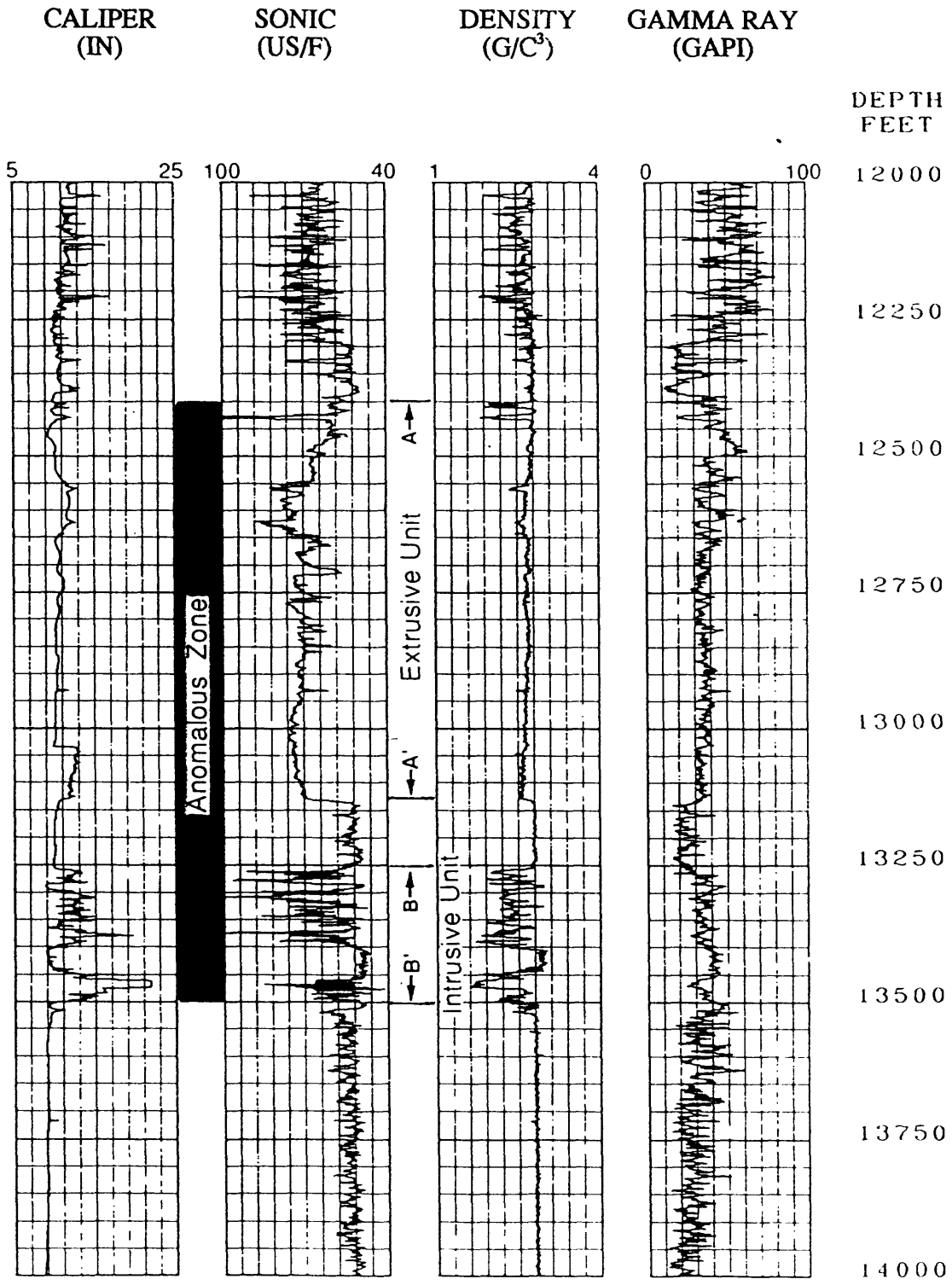

Figure 5.--Various well logs at the OCS-170A well site for the anomalous interval. The interval A-A' is a sequence of weathered extrusive volcanics. The underlying B-B' interval is a volcanic intrusive unit.

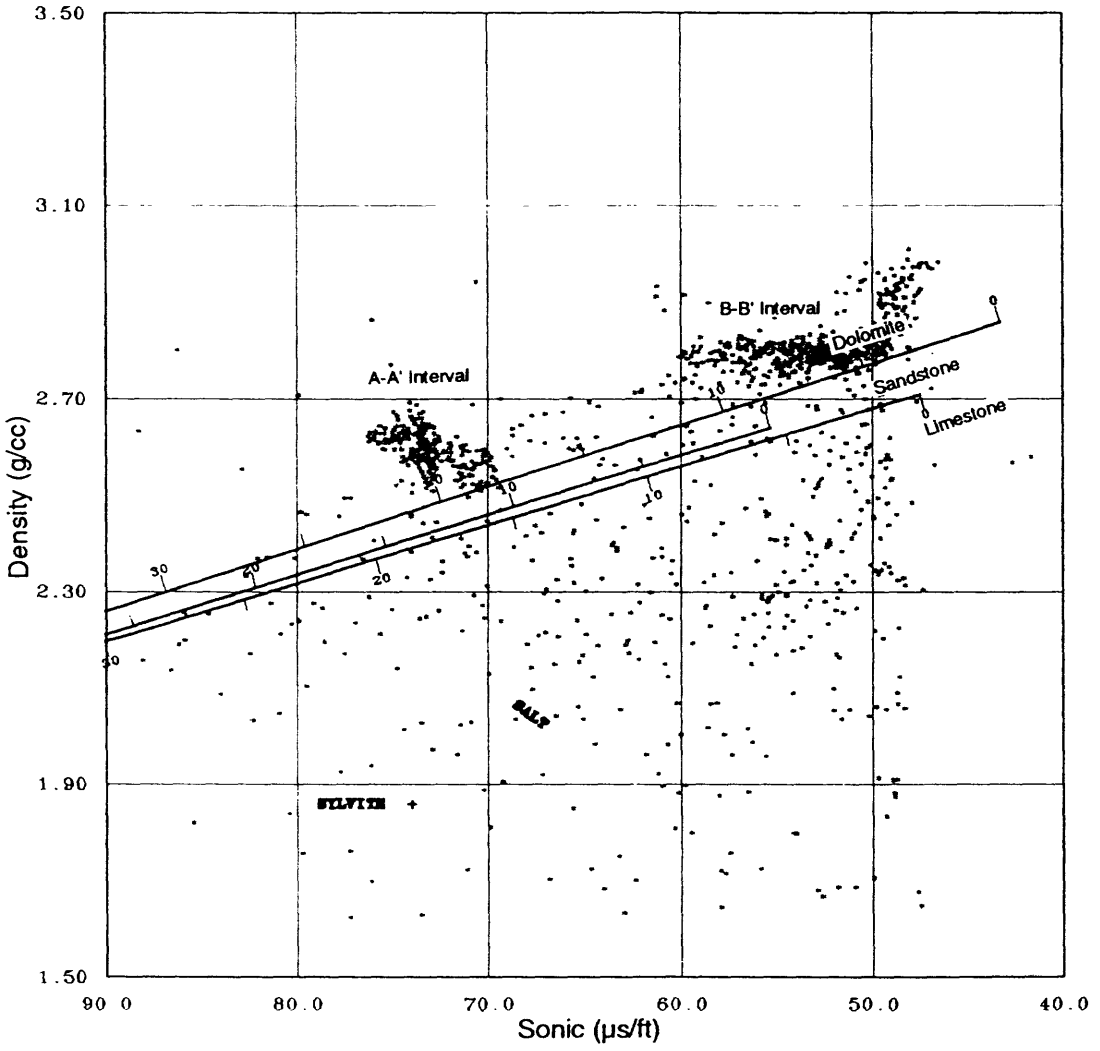

Figure 6.--Cross-plot between sonic and density log values over the anomalous interval showing a mean density of about 2.65 g/cc and average velocity of 4.4 km/s (14291 ft/s) for the weathered extrusives and a mean density of about 2.7 g/cc and average velocity of 6.2 km/s (20446 ft/s) for the volcanic intrusive unit. Limestone intervals show typical density values of about 2.7 g/cc and average velocities of about 5.7 km/s (18900 ft/s).

Checkshot data from the well are shown in Table 1 and indicate interval velocities of 5.3 km/s (17241 ft/s) for the **A-A'** sequence and 5.4 km/s (17857 ft/s) for the **B-B'** sequence. Averaged interval velocities derived from the checkshot data, sonic log, and stacking velocities are shown in Figure 7. Over the anomalous interval, both the velocities from the sonic log and the stacking velocities are about 300 - 600 m/s (1000 - 2000 ft/s) slower than the averaged interval velocities derived from the checkshot data leading us to suspect the accuracy of the checkshot data.

Synthetic Seismograms & Interpretation

To aid in the identification of various reflecting horizons, synthetic seismograms were generated by convolving a filtered wavelet with a series of reflection coefficients calculated from the sonic log with the assumption of constant density. The use of constant density is considered a valid practice since density affects the resulting reflection coefficients by only a small amount. Using the available checkshot data, we corrected the depth values of the sonic log and generated a corresponding synthetic seismogram, but the results were unsatisfactory. Because of the large differences between the sonic log and checkshot data, the checkshot-corrected synthetic seismograms exhibited numerous artifacts. Such artifacts are described in detail by Lee and others (1991). Correlations were considered fair in the upper 2 seconds but deteriorated considerably thereafter. Therefore, we opted to use only the first checkshot data point to correct the sonic log depths and the resulting synthetic seismograms correlated much better with the actual seismic data. Using the same depth correction procedures, and sonic log, we generated the synthetic vertical seismic profile (VSP) shown in Figure 8. The synthetic VSP is bandpass filtered at 6/10-42/56 Hz. Bandpass filters used for synthetic seismograms (Figure 8 **a-d**) were 6/10-68/96 Hz, 6/10-50/68 Hz, 6/10-42/56 Hz, and 6/10-32/42 Hz, respectively. In Figure 8, the peak labeled **A** is a reflection from the boundary between calcareous shale and limestone. The boundary between limestone and the middle Jurassic extrusive unit (**A-A'** sequence) produces a reflection shown as a trough, labeled **B**. The strong peak labeled **C** is interpreted to be a reflection from the boundary between the base of the extrusive unit and limestone. Both low and high impedance segments exist within the intrusive volcanic rocks. A reflection from the top of the low impedance segment of the intrusive unit (**B-B'** sequence) is shown as a strong trough, labeled **D**, while the reflection from the high impedance segment is shown as another peak, labeled **E**. Apparent reflection coefficients for horizons **A-E** filtered at 6/10-32/42 Hz were calculated to be 0.09, -0.1, 0.14, -0.11, and 0.06 respectively.

A segment of line 12 at an expanded scale is shown in Figure 9 along with a bandpass filtered (6/10-32/42 Hz) synthetic seismogram inserted at the location of the anomaly. Correlation for events **C-E** between synthetic and surface seismic data is good. However, the broad peak at **A** and subsequent trough at **B** are not observed on the actual recorded data. Possible sources for this mismatch will be addressed later.

Inversion

Inversion of a seismic trace is in essence the reverse of the procedure that is used to create synthetic seismograms using borehole sonic logs. By using seismic trace amplitude and phase information, and using a constant bulk density for sub-bottom sediments, inversion theory can be used to get detailed estimates of interval velocities (Lindseth, 1979; Cook and Schneider, 1983).
In order for this procedure to work however, the seismic trace must be processed with wavelet deconvolution and relative true-amplitude recovery. Since surface multichannel seismic-reflection data is typically recorded in the 6 to 100 Hertz (Hz) range, inversion provides only band-limited impedances, or velocities, producing only local high frequency variations. By including information from detailed velocity analysis (e.g. stacking velocities) to obtain the missing low-frequency

Depth (feet)	One-way traveltime (ms)
0.0	0.0
2316.93	382.00
3017.06	461.00
3517.06	519.00
4017.06	574.00
4416.99	618.00
4916.99	668.00
5416.99	716.00
5916.99	757.00
6416.99	797.00
6916.99	844.00
7416.99	884.00
7816.93	917.00
8416.99	964.00
8916.99	1000.00
9416.99	1039.00
9916.99	1073.00
10416.99	1109.00
10916.99	1143.00
11416.99	1177.00
11916.99	1206.00
12276.90	1228.00
12517.06	1245.00
12756.89	1261.00
13017.06	1274.00
13267.06	1288.00
13517.06	1302.00
13766.40	1316.00
14023.62	1335.00
14267.06	1347.00
14517.06	1360.002

Table 1. Checkshot data from well OCS170-A (EX133-1)

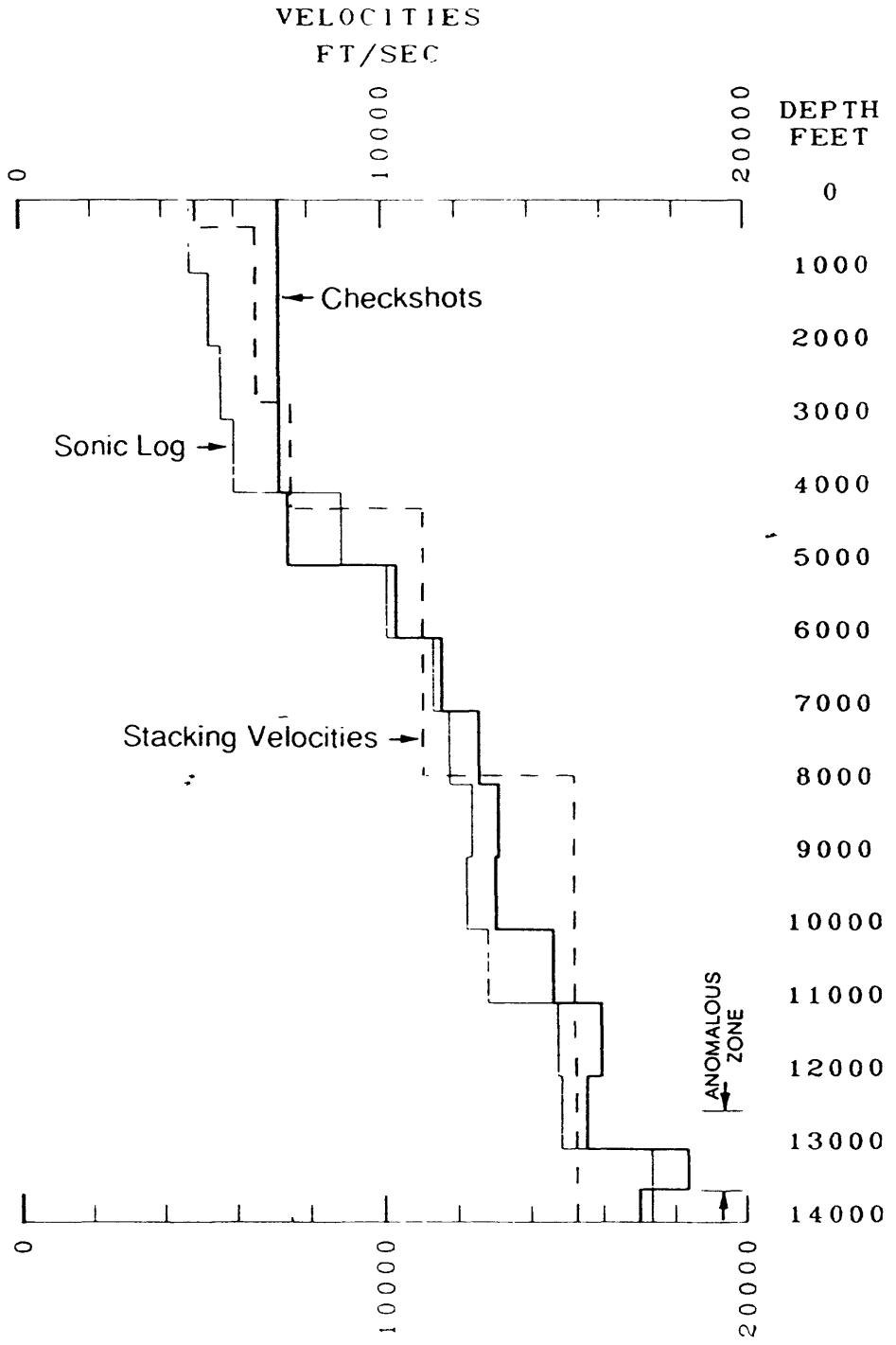

Figure 7.--Plot showing averaged interval velocities derived from checkshot data, sonic log, and stacking velocities.

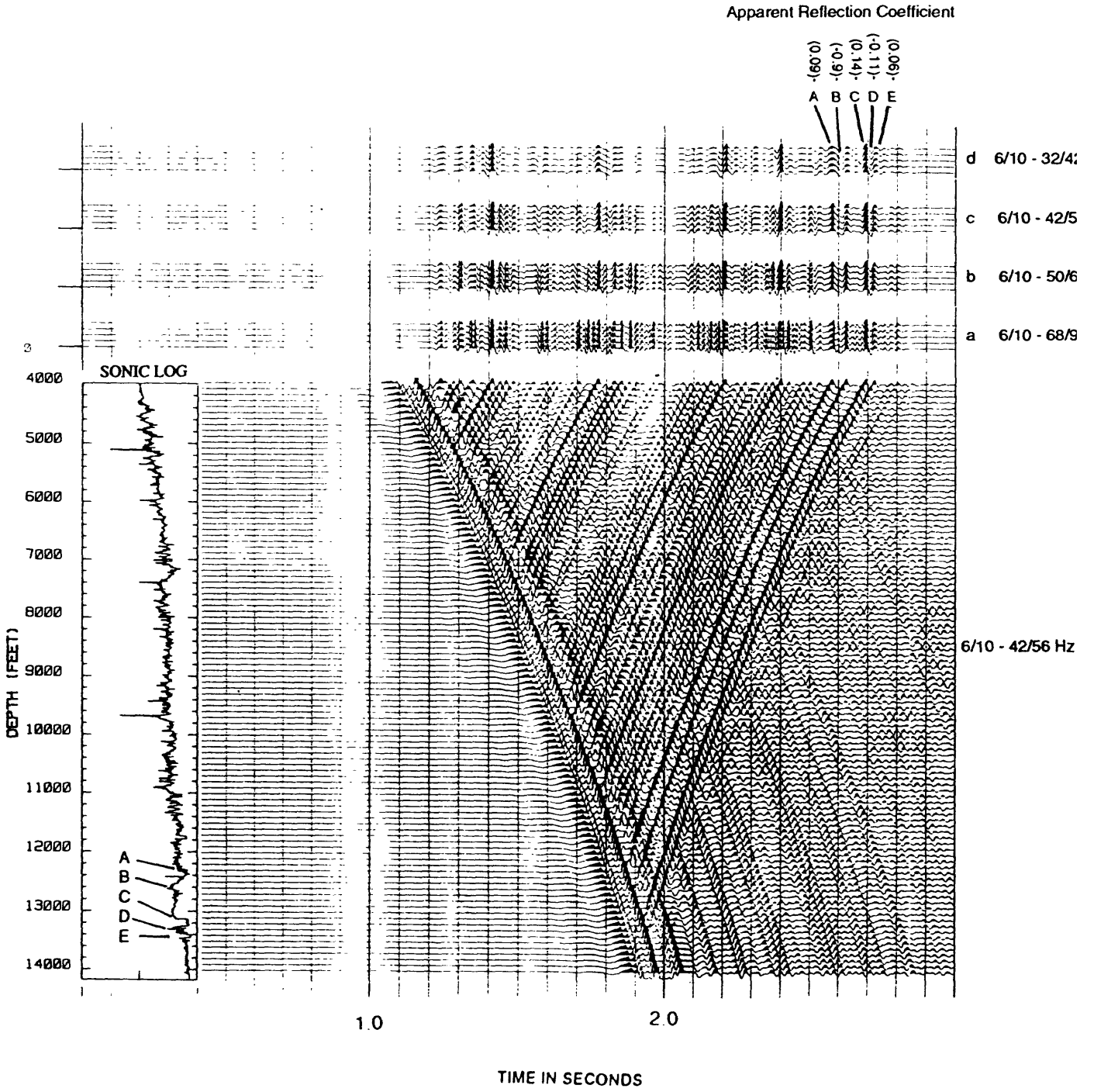

Figure 8.--Synthetic vertical seismic profile (VSP) for the OCS-170A well, bandpass filtered at 2/10-42/56 Hz. Apparent reflection coefficients for events marked A-E are 0.9, -.1, .14, -.11, and .06 respectively. Synthetic seismograms a-d were filtered at 6/10-68/98 Hz, 6/10-50/68 Hz, 6/10-42/56 Hz, and 6/10-32/42 Hz respectively.

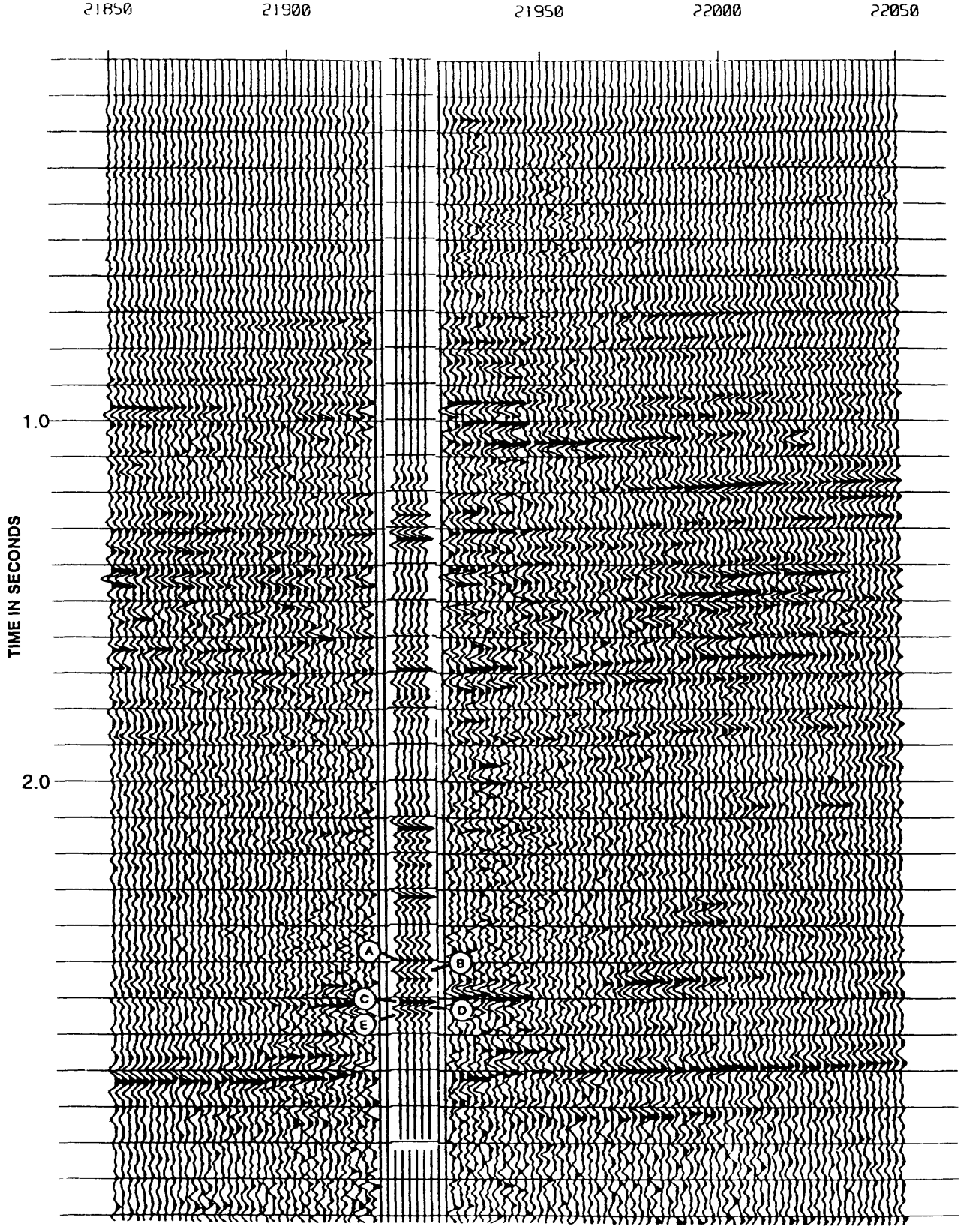

Figure 9.--Expanded segment of USGS line 12 over the anomalous zone associated with the volcanic units. Inset is a synthetic seismogram using the sonic log from OCS-170A. Horizons marked A-E correlate with those of Figure 8.

component of velocity, Lindseth (1979) described a method to get absolute interval velocity values.

Using an apparent reflection coefficient of 0.14 for the top of the anomalous zone as seen on the surface seismic data, and a starting velocity model derived from stacking velocities, we inverted the seismic data for interval velocities using the "**STRATA**" software package from Hampson & Russell and the results are shown in Figure 10. The anomaly is shown between CMPs 21910 and 21950 at about 2550 milliseconds (ms). The interval velocity for the anomaly shown as green between CMPS 21910 - 21945 is between 4.4 km/s and 4.5 km/s, providing a good match with the sonic log data values for the interval **A-A'** in figure 5. We interpret this low velocity zone to be the base of the extrusive unit.

Discussion

As previously noted, with the exception of events **A** and **B**, the synthetic seismograms provide a good match to the surface seismic data (Figure 9). Inaccuracies resulting from bad or inaccurate density values, sonic values, checkshot data values, or numerous other reasons (Balch and Lee, 1984) could account for bad correlations in certain portions of the seismogram. However, since horizons above, below, and even within the anomalous zone show a good correlation between the synthetics and the seismic section, we believe that both were generated from reliable data and are free of any gross processing artifacts. Therefore, the absence of horizons **A** and **B** on the seismic section must result either from an effect or combination of effects that produce(s) a different response when sampling in 1-D, as represented by the sonic well-log and the resulting seismogram, versus a 2- or 3-D sampling such as that represented by the surface seismic section.

Reflections on seismic sections and synthetic seismograms occur when impedance contrasts exist between layers, and the amplitudes of the reflections vary proportionately with the impedance contrasts. Synthetic seismograms rely only on information gathered in the immediate vicinity of a well. They essentially provide information from only one dimension (depth). Impedance contrasts are assumed to come from discrete, flat, isotropic layers that are infinitely long. No assumptions are made with regard to any two- or three-dimensional effects.

A decrease in the signal to noise ratio (S/N) in an area of a seismic section results in decreasing trace amplitudes and a loss of lateral coherency. Possible sources for a loss in signal to noise ratio are, 1) a decrease in fold, 2) water bottom scatterers, 3) a deterioration in source signal strength, and 4) inaccurate stacking velocities. The signal to noise ratio theoretically increases as the square root of the fold. Because of missing shots, our data set decreases in fold over the anomalous zone from 48 to 37 thus decreasing the theoretical signal to noise ratio from 6.9 to 6.1. This kind of amplitude loss however, is usually not time dependent. Horizons above and below the two missing horizons **A** and **B** are recognizable. Therefore, we can argue that the absence of horizons **A** and **B** on our seismic section is not due to a low signal to noise ratio or to a processing artifact. This same time independent argument can be made for both water bottom scatterers and losses in source signal strength. Stacking CMPs with inaccurate velocities may also lead to a decrease in amplitude strength. Careful velocity analyses in the anomalous zone assured us that we were attaining the optimum stacking response.

Knapp (1991) showed how the seismic response behaves in a number of Fresnel zones for broadband data. From small targets, one can have decreases in the seismic response amplitudes at places where diffractions interfere destructively with primary reflections. This phenomenon typically occurs when the ratio between the target radius and its depth is very small (<= .05). Figure 11 shows the seismic amplitude response of a circular disk of varying radius buried at a depth of 500 m using a 25 Hz Ricker "source" wavelet. The increase in amplitudes within the first Fresnel zone is due to constructive interference.

Hilterman (1970) showed how the modeled seismic amplitude response resulting from a line recorded over a three-dimensional feature changes as the line deviates from the center of the feature.

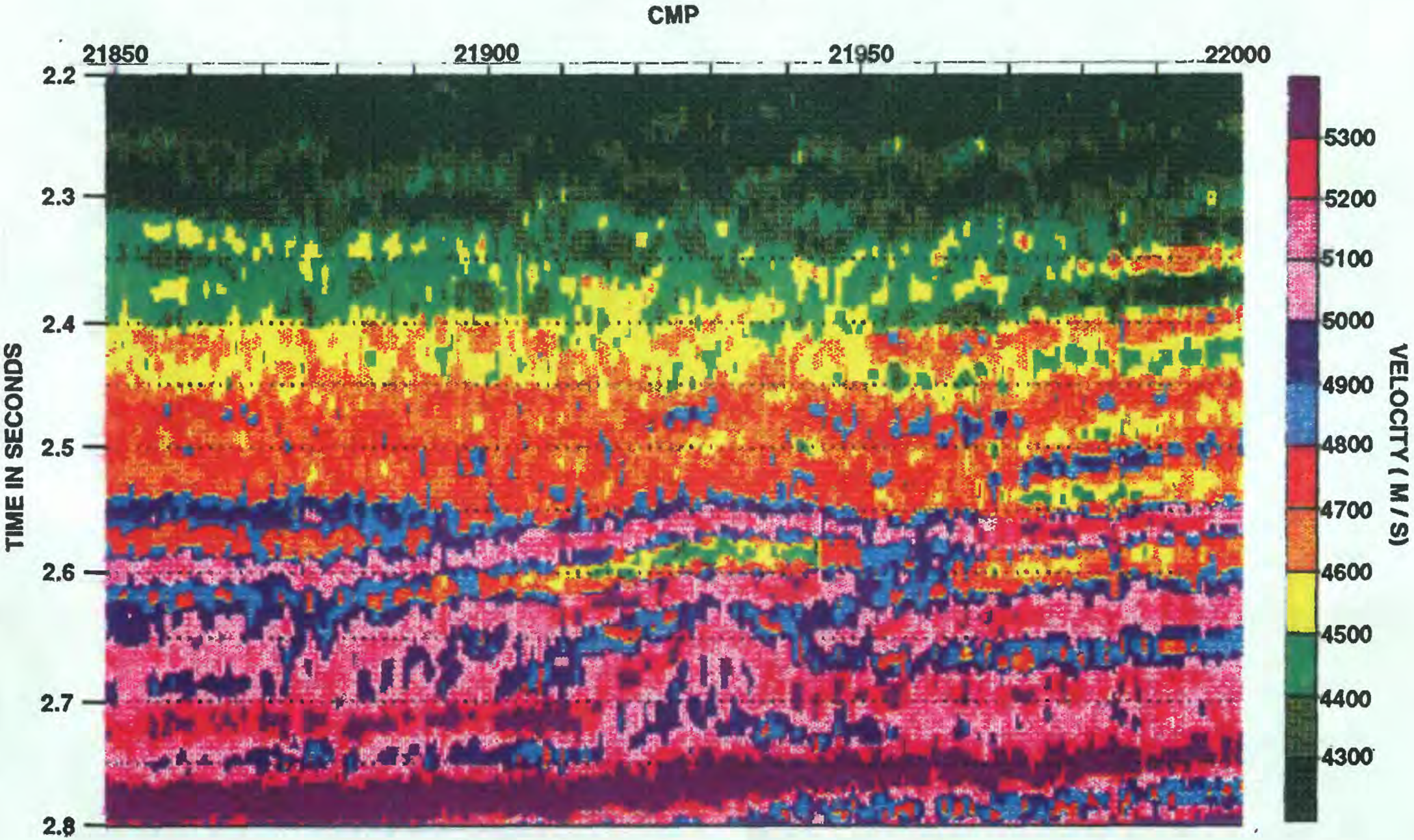

Figure 10.--Interval velocities from inversion of the data over the anomalous zone using software from Hampson & Russell Services, LTD. Results show the anomalous zone having an interval velocity between 4.4 km/s and 4.5 km/s.

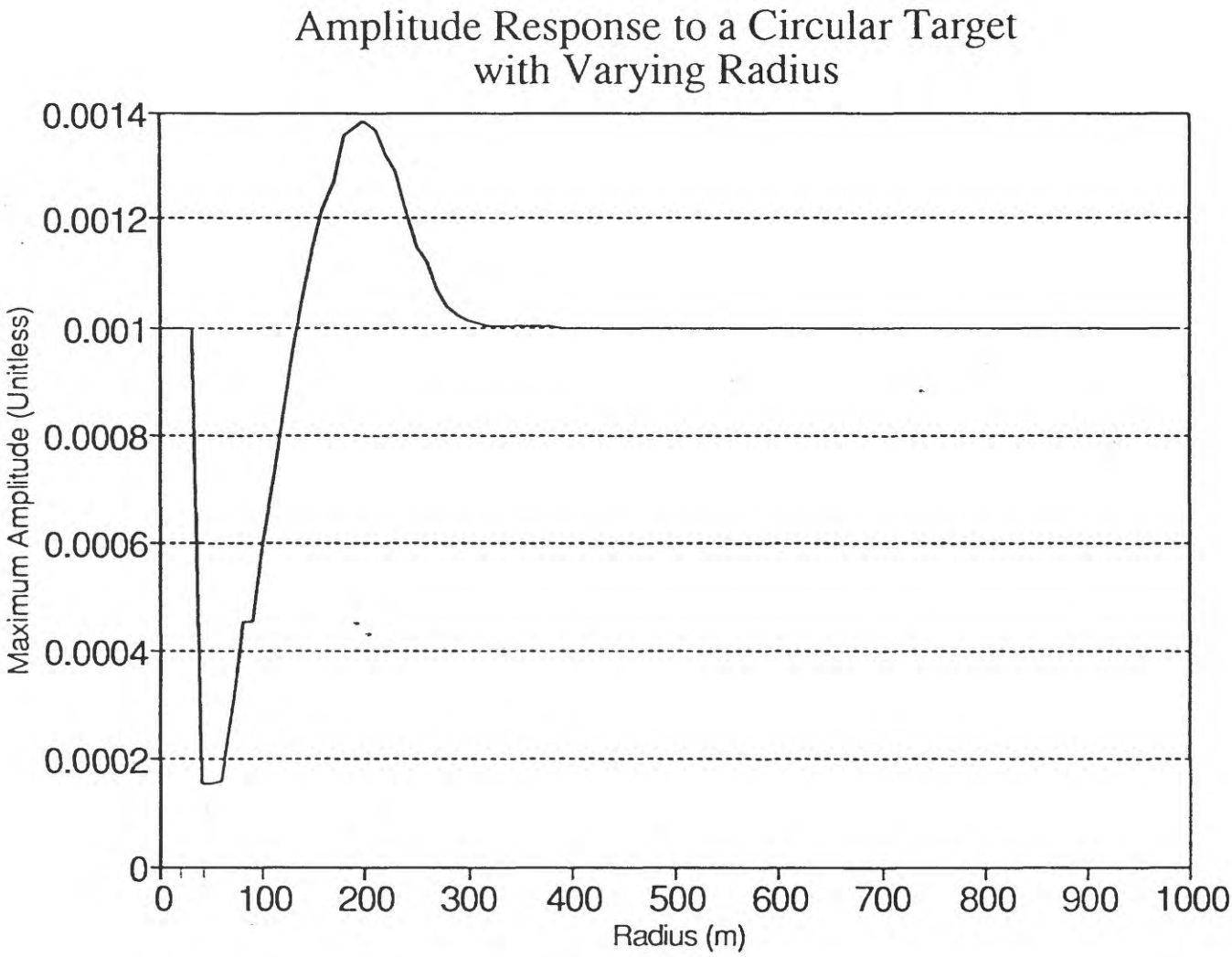

Figure 11.--Seismic response of a reflector of varying radius buried at a depth of 500 m. With a radius/depth to target ratio less than about .05, diffractions destructively interfere with primary reflections.

Based on a three-dimensional feature's position relative to a seismic line, Lee (1986) investigated side echo problems encountered in the interpretation of multichannel seismic data over craters created by nuclear blasts at Enewetak atoll in the Marshall Islands (Grow and others, 1986). Figure 12a is the seismic response of a line centered over a 3-dimensional symmetrical horst model. Figure 12b is the response from the same model with the line offset 25 m from the center of the anomaly based on the computational method described by Lee (1986). Reflection amplitudes from the top of the horst block in Figure 12b are half as large as those of Figure 12a. This again shows how the existence of a primary reflection can be masked by effects from outside the plane of interest i.e., three-dimensional effects.

A combination of the effects described in the previous two paragraphs allows us to suggest that the anomaly present in our seismic section arises from varying lithologies over a relatively small lateral extent. The schematic shown in Figure 13 describes one possible interpretation of the anomaly and correlates well with our data set and the information from the well logs. This interpretation allows for laterally varying lithologies along the upper boundary of the anomaly where relatively small, localized blocks of limestone are juxtaposed with the extrusive unit. This configuration would explain how the seismic reflections at the locations marked as **A - E** in Figure 9 would appear in a synthetic seismogram while simultaneously, because of the previously mentioned 3-D phenomena, the locations marked as **A** and **B** would be missing on the actual surface seismic data.

A secondary goal of our paper was to assess our ability to use surface seismic data to distinguish between various lithologies, particularly intrusive salts and weathered volcanics, both of which are found in the Georges Bank basin region. Inversion results from Lee and others (1990) showed the intrusive salt layer to have a P-wave velocity of about 4.0 km/s (13123 ft/s). Results from this study suggest a P-wave velocity for the weathered volcanics of about 4.45 km/s (14600 ft/s). With these velocities, reasonable density values, and knowledge of the rock containing these layers, we can calculate normal incidence reflection coefficients. Using densities 2.2 g/cc for the salt and 2.55 g/cc for the weathered volcanics, and assuming that these layers are encased in a high impedance layer(P-wave velocity 5.8 km/s, density 2.7 g/cc), the calculated normal incidence reflection coefficients would then be -.28 and -.165 for the salt and weathered layers respectively. Such a difference in reflection coefficients (almost 2:1) may be detectable with relative true amplitude processing. The two anomalies shown in Figure 3 suggests such an amplitude difference.

Another reflection seismic method for differentiating between two lithologic environs is through the use of amplitude versus offset (AVO) analysis. Figure 14 shows how the difference in reflection coefficients changes with angle of incidence using the velocities and densities shown in Table 2. Curves **a-c** result when going from the low impedance layer(s) to a high impedance layer and curves **a'-c'** result when going from the low impedance layer(s) to a high impedance layer. The curves for the intrusive salt and the weathered volcanics are not separated enough to be detectable in the presence of noise. Even with changes in the S-wave velocity for the weathered volcanics layer, the curves do not separate enough to enable us to distinguish between the two anomalous zones with confidence.

Conclusions

From our analysis and interpretation of the anomaly located between CMPs 21900 and 22000 of USGS line 12, we conclude the following:

1) The anomaly is the seismic response of a three-dimensional feature at least 3 km in diameter. The feature is comprised of two low-impedance layers (volcanic layers) overlain and separated by high-impedance layers (limestone units).

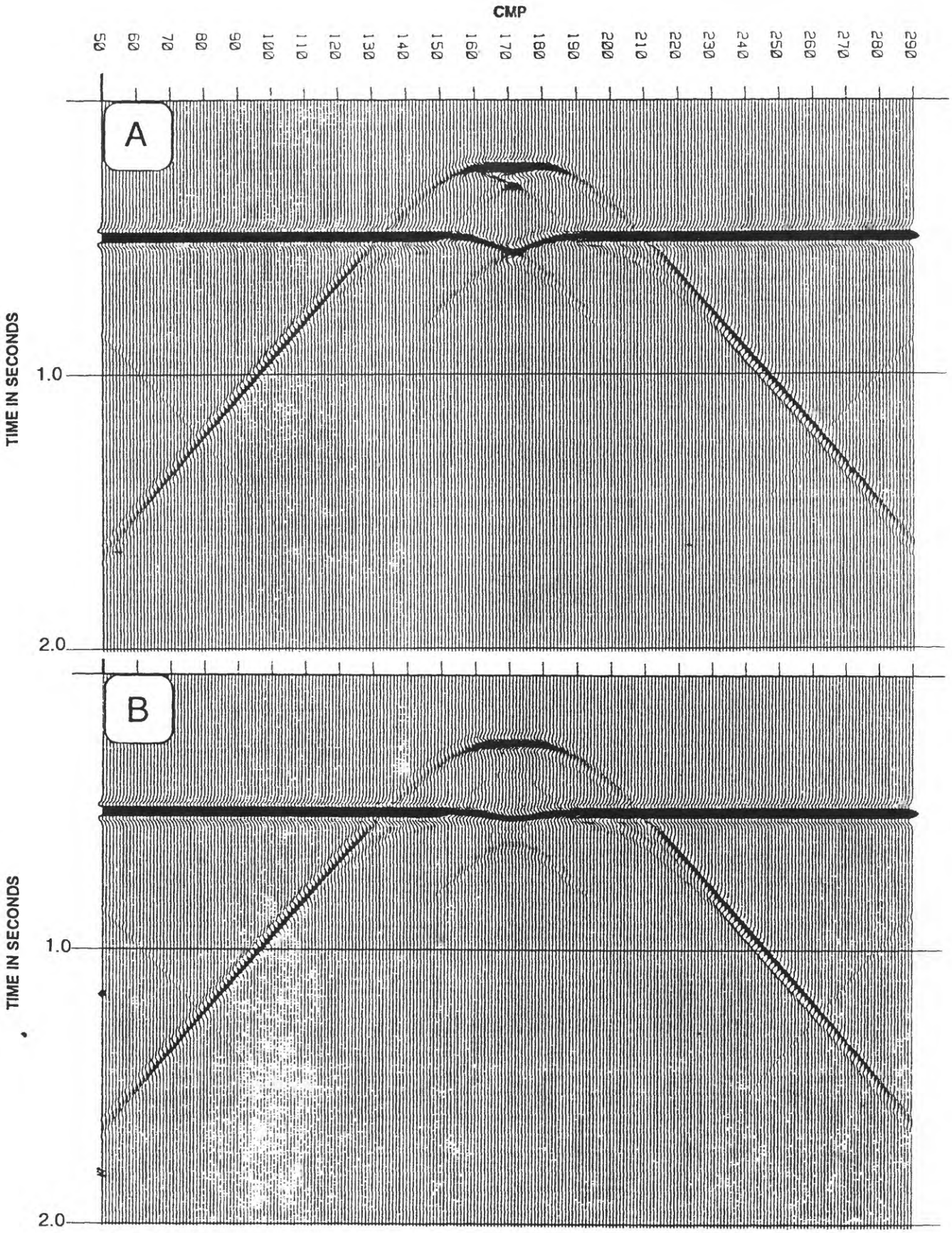

Figure 12.--Seismic response of a line crossing over a 3-dimensional, symmetric horst block. The response shown in A is the result from the line crossing directly over the center of the block. The response shown in B resulted from the line crossing 25 m (1 Fresnel zone) from the center of the block.

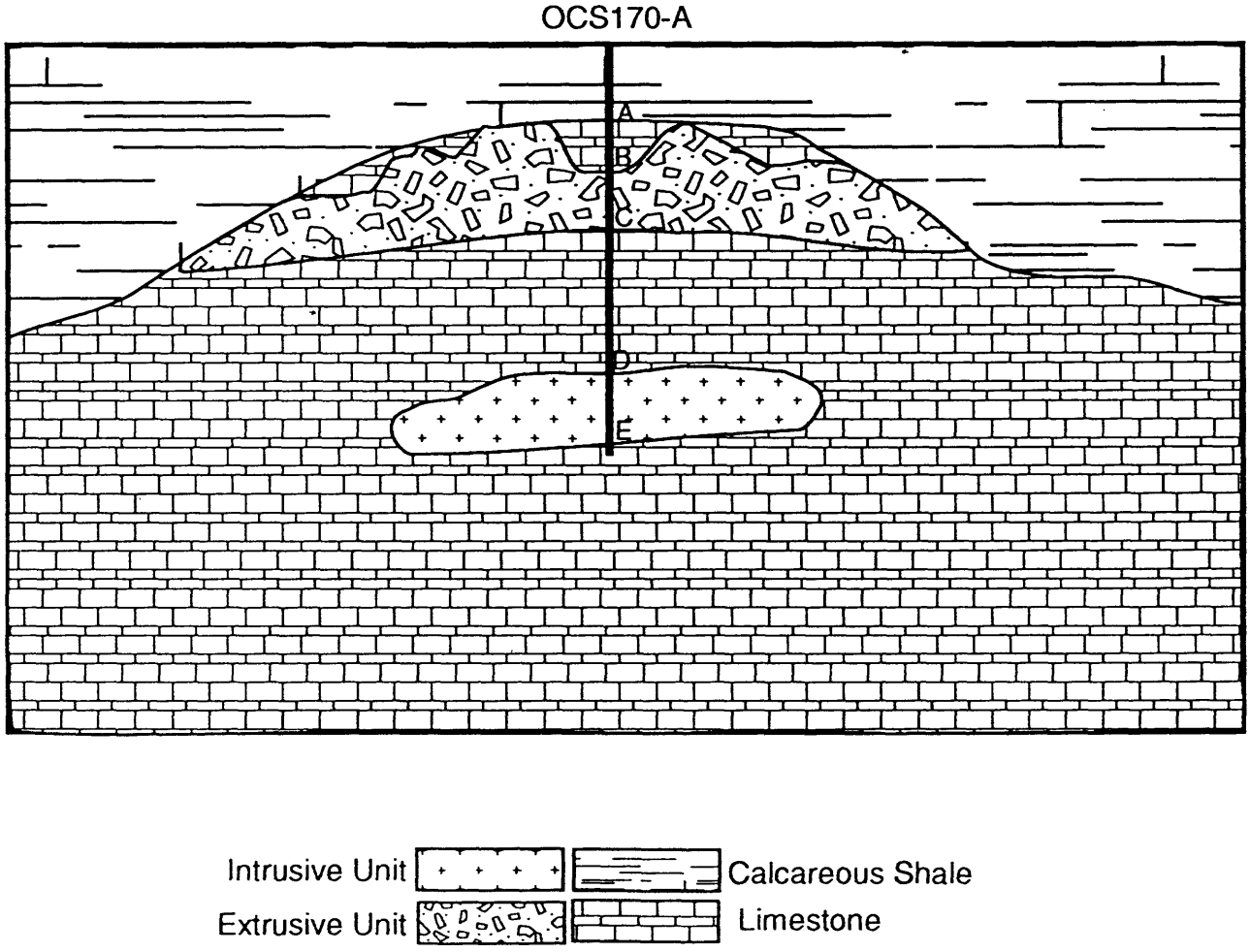

Figure 13.--Schematic cross-section of one possible interpretation of the anomalous zone.

Layer	Velocity (km/s)		Density (g/cc)
	P-Wave	S-Wave	
High impedance background	5.8	3.0	2.7
a - Volcanics (high S-wave velocity)	4.1	1.9	2.55
b - Volcanics (low S-wave velocity)	4.1	1.6	2.55
c - Salt	4.3	2.1	2.2

Table 2. Velocity and density values used for calculating Figure 14

2) The top of the anomalous zone with an overall appearance as a low impedance zone actually contains areas of highly localized blocks of high impedance rocks (limestone) juxtaposed with a low impedance unit (weathered extrusives). These blocks are not resolved on the surface seismic data because of Fresnel zone and 3-dimensional effects.

3) Inversion of our surface seismic data for velocities yielded values that are consistent with sonic log values and with our interpretation.

4) With relative true amplitude processing, and by analyzing reflection amplitude differences, it is feasible to differentiate between the intrusive salts and the weathered volcanics found in the study area.

5) Theoretical AVO curves show that it would be difficult to differentiate between intrusive salts and weathered volcanics with AVO analysis alone. Actual AVO analysis was not performed because of the lack of detailed source- and hydrophone-array information and non-uniform channel sensitivity.

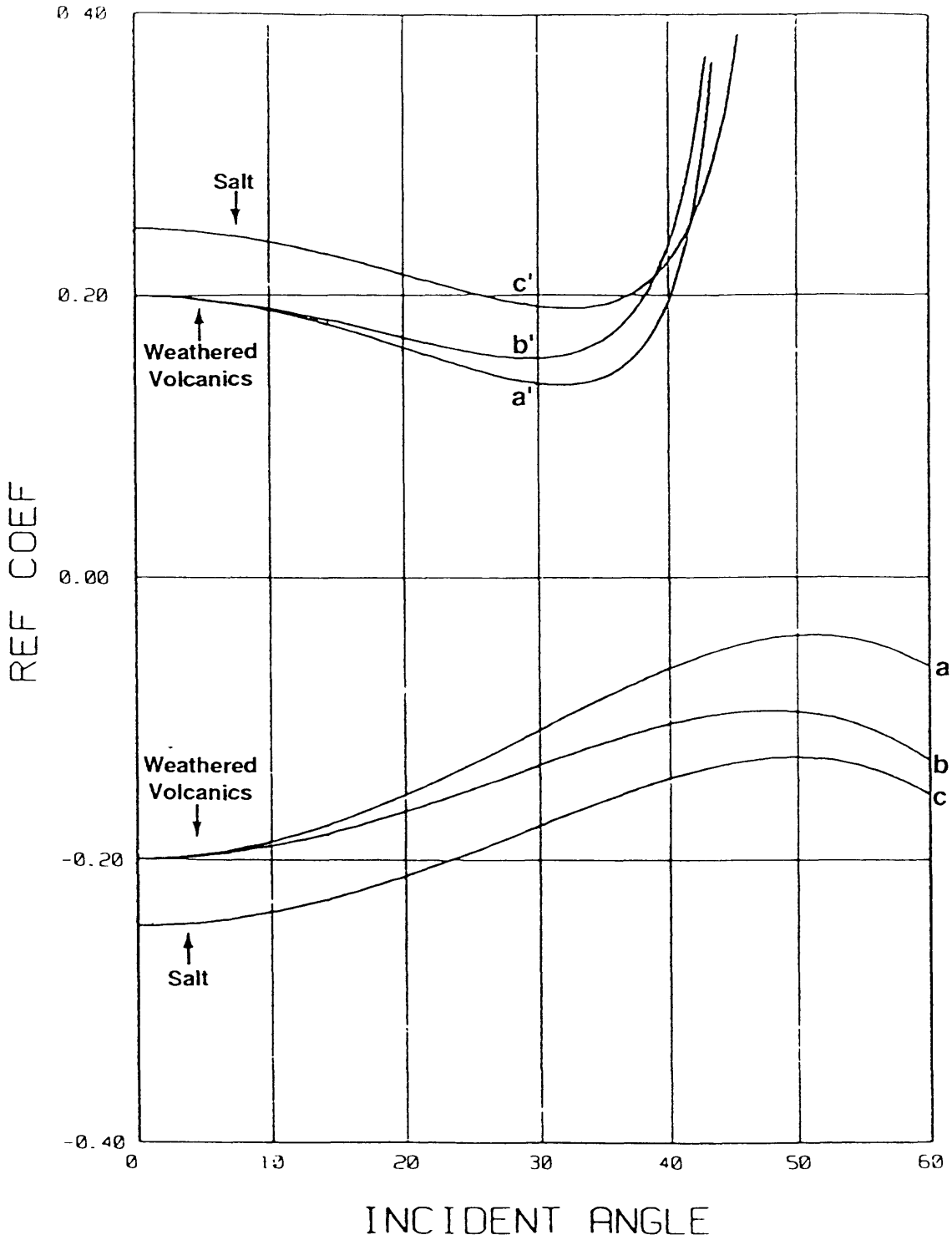

Figure 14.--Reflection coefficient versus incident angle for a low impedance layer (salt or weathered volcanics) encased in a high impedance layer. Curves **a** and **b** show the response from the weathered volcanics with shear wave velocities of 1.9 km/s and 1.6 km/s respectively. Curve **c** shows the response from the salt layer. The upper curves represent the response from the bottom of the low impedance layer, and the lower curves are from the top.

References

Anderson, R. C. and Taylor, D. J., 1981, Very high amplitude seismic anomaly in Georges Bank Trough, Atlantic continental margin: The American Association of Petroleum Geologists Bulletin, vol. 65, p. 133-144.

Backus, M. M., 1987, Amplitude versus offset: A review: Society of Exploration Geophysicists 57th annual international meeting and exposition, Oct. 11-15, New Orleans, Expanded abstracts, p. 359-364.

Balch, A. H., and Lee, M. W., 1984, Vertical Seismic Profiling - Technique, Applications, and Case Histories: Boston, International Human Resources Development Corporation, 488 p.

Cook, D.A., and Schneider, W.A., 1983, Generalized linear inversion of reflection seismic data: Geophysics, v. 48, p. 665-676.

Emery, K. O., and Uchupi, E., 1972, Western North Atlantic Ocean, Topography, rocks, structure, water, life, and sediments: American Association of Petroleum Geologists, Memoir 17. 532p.

Gray, W. C., 1979, Variable norm deconvolution: Palo Alto, CA, Stanford University Ph.D. Thesis.

Grow, J. A., Lee, M. W., Miller, J. J., Agena, W. F., Hampson, J. C., Hester, D. S., and Woellner, R. A., 1986, Multichannel seismic-reflection survey of KOA and OAK craters, in Folger, D. S., Sea-floor observations and subbottom seismic characteristics of OAK and KOA craters, Enewetak Atoll, Marshall Islands: U. S. Geological Survey Bulletin 1678, p. D1-D46.

Hilterman, F. J., 1970, Three-Dimensional Seismic Modeling: Geophysics, v. 35, no. 6, p. 1020-1037.

Hurtubise, D.O., Puffer, J.H., and Cousminer, H.L.,1987, An offshore Mesozoic igneous sequence, Georges Bank basin, North Atlantic: Geological Society of America Bulletin, v. 98, p. 430-438.

Jansa, L. F., and Wiedmann, J., 1982, Mesozoic-Cenozoic development of the eastern North American and Northwest African continental margins: A comparison, in VonRad, U., Hinz, K., Sarnthein, M., and Seibold, E., eds. Geology of the northwest African continental margin: New York, Springer-Verlag, p. 215-269.

Knapp, R. W., 1991, Fresnel zones in the light of broadband data: Geophysics, v. 56, no. 3, p. 354-359.

Lee, M. W., 1986, Seismic Responses for Circularly Symmetrical Bodies: U. S. Geological Survey Open-File Report 86-553, 18 p.

Lee, M. W., and Hutchinson, D. R., 1990, True-amplitude processing techniques for marine, deep crustal reflection seismic data: U.S. Geological Survey Bulletin 1897, 22 p.

Lee, M. W., Agena, W.F., and Swift, B.A., 1991, An analysis of a Unique Seismic Anomaly in Georges Bank Basin, Atlantic Continental Margin: U.S. Geological Survey Open-File Report 91-138, 25 p.

Lindseth, R.O., 1977, Synthetic soniclogs--a process for stratigraphic interpretation: Geophysics, v. 44, p. 3-26.

Manspeizer, W., Puffer, J. H., and Cousminer, H. L., 1978, Separation of Morocco and eastern North America; A Triassic-Liassic stratigraphic record: Geological Society of America Bulletin, v. 89, p. 901-920.

Schlee, J. S., Mattick, R. E., Taylor, D. J., Girard, O. W., Grow, J. A., Rhodehamel, E. C., Perry, W. J., Jr., Bayer, K. C., Furbush, M., Clifford, C. P., and Lees, J. A., 1975, Sediments, structural framework, petroleum potential, environmental conditions, and operational considerations of the United States North Atlantic outer continental shelf: U. S. Geological Survey Open-File Report 75-353, 179 p.

Poag, C.W., 1982, Stratigraphic reference section for Georges Bank Basin - Depositional model for New England passive margin: American Association of Petroleum Geologists Bulletin, v. 66. p. 1021-1041.

Schlee, J. S., Behrendt, J. C., Grow, J. A., Robb, J. M., Mattick, R. E., Taylor, P. T., and lawson, B. J., 1976, Regional geologic framework off northeastern United States: AAPG Bulletin, v. 60, p. 926-951.

Schlee, J. S., Martin, R.G., Mattick, R. E., Dillon, W. P., and Ball, M. M., 1977, Petroleum geology on the United States Atlantic-Gulf of Mexico margins: Exploration and economics of the petroleum industry, v. 15, p. 47-93: New York, Matthew Bender and Co., Inc.

Simonis, E. K., 1980, Lithologic description, in Amato, R. V., and Simonis, E. K., eds., Geologic and operational summary COST No. G-2 well, Georges Bank area, North Atlantic OCS: U.S. Geological Survey Open-File Report 80-269, P. 14-19.